

Density dependence of the $\nu = \frac{5}{2}$ energy gap: Experiment and theory

J. Nuebler,¹ V. Umansky,² R. Morf,³ M. Heiblum,² K. von Klitzing,¹ and J. Smet¹

¹Max-Planck-Institute for Solid State Research, Heisenbergstr. 1, D-70569 Stuttgart, Germany

²Braun Centre for Submicron Research, Department of Condensed Matter Physics, Weizmann Institute of Science, Rehovot 76100, Israel

³Condensed Matter Theory, Paul Scherrer Institute, CH-5232 Villigen, Switzerland

(Received 23 June 2009; revised manuscript received 16 November 2009; published 11 January 2010)

A density-tunable GaAs-AlGaAs heterostructure is used to study the density dependence of the filling factor $\nu = \frac{5}{2}$ and other fractional and reentrant integer quantum-Hall states in the second Landau level. The activation energy at $\nu = \frac{5}{2}$ can be determined for densities between 1.3 and $2.7 \times 10^{11}/\text{cm}^2$ and reaches up to 310 mK. The $5/2$ energy gap is calculated numerically, including finite width and Landau-level-mixing corrections, both as a function of electron density. The discrepancy between theory and experiment increases moderately with density and reaches about 1.5 K at the highest density. We argue that the activation energy is strongly influenced by disorder from ionized donors and attribute this to the surprisingly large size of the $5/2$ quasiparticles. We find that the quasiparticles have a diameter of at least 12 times the magnetic length or 150 nm at a magnetic field of 4 T. Implications for heterostructure design are discussed.

DOI: [10.1103/PhysRevB.81.035316](https://doi.org/10.1103/PhysRevB.81.035316)

PACS number(s): 73.43.Qt, 73.63.Hs

I. INTRODUCTION

Currently, there exists a strong interest in the filling factor $\nu = \frac{5}{2}$ fractional quantum-Hall effect (FQHE),^{1,2} both in theory^{3–17} and experiment.^{18–25} This is due to evidence that the Pfaffian wave function²⁶ may describe this FQHE state.^{14,15,27–29} Its $e/4$ charged excitations obey non-Abelian statistics, such that topological quantum computation might become possible by braiding these excitations (for a review see Refs. 30 and 31). However, other candidate wave functions have also been proposed with quasiparticles that do not possess non-Abelian statistics (for example, see, Ref. 6).

To identify the true nature of the $5/2$ state, a braiding experiment which demonstrates non-Abelian statistics would be compelling. Even though steps are taken in this direction,^{18,24,25} the experimental implementation is challenging. Meanwhile, other properties of the $5/2$ state can be examined experimentally. An important step in this context was the verification that the measured quasiparticle charge is compatible with the predicted value $e/4$ for the Pfaffian.^{23,24} Another actively investigated issue is the energy gap $\Delta_{5/2}$.^{2,12,19–22,32–35} This gap plays an important role as observing the $5/2$ state and possible non-Abelian physics requires thermal energies well below the gap. Even in the very best heterostructures available today $\Delta_{5/2}$ is masked to a large extent by disorder. Hence, it is crucial to identify critical sample parameters that yield the largest possible gaps. Density-tunable heterostructures are very appealing as they allow to investigate the energy gap as a function of carrier density for a given bare disorder potential. Here, we carried out such a study on a state-of-the-art heterostructure with an *in situ* grown backgate (BG). In contrast to a previous study,³⁴ the sample shows a well-developed $\nu = \frac{5}{2}$ state. In order to compare the density dependence of the $5/2$ energy gap with theory, we numerically calculate the expected gap from exact diagonalization of finite systems. We quantitatively include corrections due to finite width of the wave function and Landau-level (LL) mixing. LL mixing turns out to be the dominant effect. A comparison of the theoretical

prediction with our experimental activation energies suggests that disorder from remote ionized (RI) donors is responsible for a large part of the observed discrepancy. This conclusion is drawn based on a theoretically calculated lower bound of the size of the $5/2$ quasiparticles. Their spatial extent is surprisingly large. We estimate their size to be ≥ 12 magnetic lengths or 150 nm at 4 T. This is larger than the length scale of the disorder from ionized donors in our sample. A quantum-tunneling model, which has been invoked previously to describe the influence of disorder in the integer quantum-Hall regime in a more rigorous manner than just by static disorder level broadening,³⁶ has provided guidance to come to this conclusion. We discuss implications for the interpretation of experiments as well as the heterostructure design.

II. EXPERIMENTAL RESULTS

A. Sample

Studies were performed on a 400- μm -wide hallbar patterned on a GaAs/AlGaAs heterostructure. An *in situ* grown n^+ -GaAs layer serves as a BG to tune the electron density. The two-dimensional electron system (2DES) resides in a 30-nm-wide quantum well located 850 nm above the backgate. The well is modulation doped from the top side only using an overdoped short period AlAs/GaAs superlattice located 66 nm away from the 2DES. A homogeneously doped region closer to the surface compensates for surface depletion. Details and advantages of this doping method^{37,38} are described elsewhere.³⁹ The BG allows to tune the electron density n from complete depletion up to approximately $2.7 \times 10^{11}/\text{cm}^2$. Figure 1 depicts the electron mobility μ and the quantum lifetime τ_q as a function of n . The mobility reaches a value of $18 \times 10^6 \text{ cm}^2/\text{Vs}$ at the highest density. Above $10^{11}/\text{cm}^2$ the mobility grows linearly. At lower densities the behavior is qualitatively different. This change is also visible in the quantum lifetime τ_q extracted from Shubnikov-de-Haas oscillations at low magnetic fields where

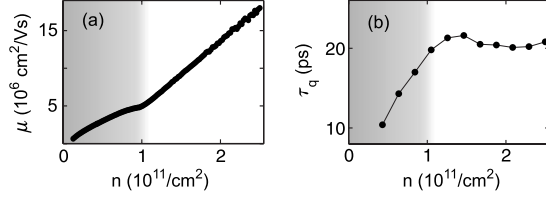


FIG. 1. Characteristic properties of our sample as a function of the electron density n . (a) Electron mobility. (b) Quantum lifetime extracted from Shubnikov-de-Haas oscillations.

spin splitting is not resolved yet. It has roughly a constant value of 20 ps above $n=10^{11}/\text{cm}^2$ but sharply drops below this density. Subsequent measurements of quantum-Hall features are performed at $n > 1 \times 10^{11}/\text{cm}^2$. The linear dependence of the mobility in this regime indicates that μ is limited by background impurities in the GaAs channel.⁴⁰ RI impurities are expected to play only a minor role for the transport mobility for this spacer thickness. Also, they would cause μ to grow superlinearly as $n^{1.5}$.^{40,41} The quantum lifetime τ_q is 200–500 times shorter than the transport lifetime τ_t calculated from the mobility in the density range above $n = 10^{11}/\text{cm}^2$. According to Ref. 42 a ratio $\tau_t/\tau_q > 10$ implies that the quantum lifetime is limited by scattering from RI instead of background impurities.

B. Second Landau-level measurements

Figure 2(a) shows the behavior of the longitudinal and Hall resistance for different densities at $T=15$ mK when the spin-up branch of the second LL is partially occupied: $2 < \nu < 3$. The FQHE features improve considerably with increasing n . The $\nu=5/2$ state [marked in Fig. 2(a) by arrows] is well resolved at $1.5 \times 10^{11}/\text{cm}^2$, $\nu=7/3$ is slightly weaker, and $\nu=8/3$ emerges at about $2 \times 10^{11}/\text{cm}^2$. Weakest, but clearly visible at the highest accessible densities are the 11/5 and 14/5 states. Apart from these FQHE states, also reentrant integer quantum-Hall-effect behavior (RIQHE) is observed near fillings $\nu=2.57, 2.44$, and 2.3. This reentrant behavior has been attributed to the formation of quantum liquid crystal phases from excess electrons or holes.⁴³ The fourth RIQHE state, observed around $\nu=2.7$ in other samples,^{21,35} is missing. Panels (b) and (c) plot the temperature dependence of the transport quantities for a density of $2.5 \times 10^{11}/\text{cm}^2$.

C. Activation gaps in the second LL

Energy gaps Δ for the observed FQHE states and the most prominent RIQHE state at filling $\nu=2.57$ are determined using $R_{xx} \sim e^{-\Delta/2k_B T}$. Exemplary Arrhenius-plots are displayed for filling 5/2 and various densities between $n=1.29$ and $2.67 \times 10^{11}/\text{cm}^2$ in Fig. 3(a). The RIQHE at $\nu=2.57$ also shows activated behavior over 2 orders of magnitude as illustrated in Fig. 3(b). Previously, only the temperature dependence of R_{xy} as well as the behavior under tilt have been studied for this reentrant state.^{21,44}

Energy gaps as a function of the electron density are shown in Fig. 3(c). Among the FQHE states 5/2 and 7/3 have the largest gaps. $\Delta_{5/2}$ reaches 310 mK at the highest density.

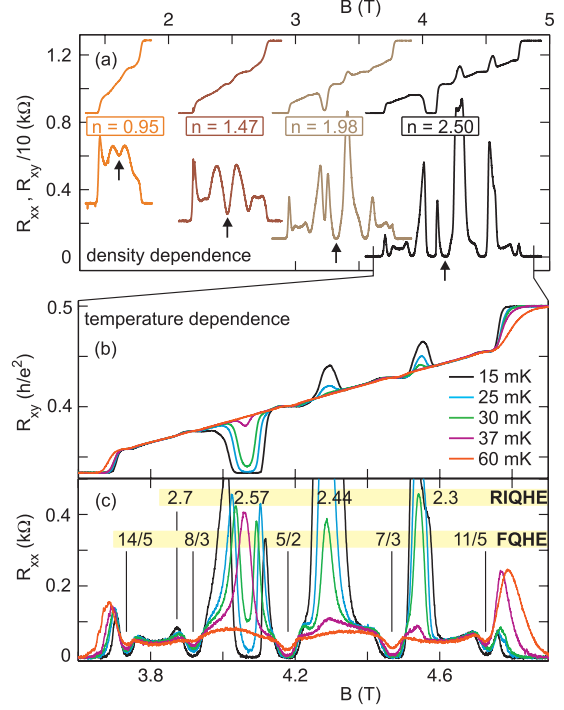


FIG. 2. (Color) Evolution of the longitudinal and Hall resistances with density and temperature, shown between $\nu=2$ and 3. (a) Density dependence of R_{xx} and R_{xy} (densities in units of $10^{11}/\text{cm}^2$). All traces are taken at 15 mK. Filling 5/2 is marked by arrows. Other filling factors can be identified by comparing with panel (c). R_{xx} traces are offset for clarity. (b) Temperature dependence of R_{xy} and (c) R_{xx} for $n=2.5 \times 10^{11}/\text{cm}^2$.

This is comparable, though less than the largest measured $\Delta_{5/2}$ to date (Ref. 22: 544 mK and Ref. 21: 450 mK). It is an open question, whether the 5/2 state is fully spin polarized. A not fully polarized state might be identified from a kink in the magnetic field dependence of the energy gap associated with a change in spin polarization. Our data shows no sign of such a spin transition but due to the limited density range we

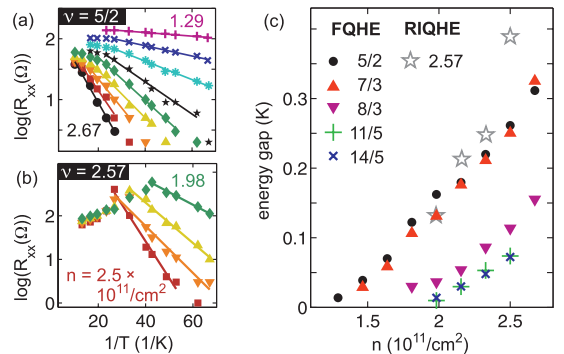


FIG. 3. (Color) Arrhenius plots for (a) the 5/2 state and (b) the reentrant integer quantum-Hall state at filling factor 2.57. Different symbols/colors correspond to different densities (examples given in units of $10^{11}/\text{cm}^2$). Activation energies are calculated from linear fits in the activated regime. (c) Density dependence of the activation energies for the fractional quantum-Hall states listed in the legend and for the $\nu=2.57$ reentrant integer quantum-Hall state.

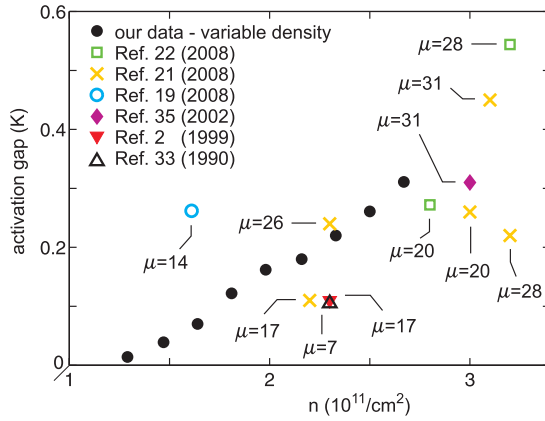


FIG. 4. (Color) Comparison of our measured $5/2$ gaps to literature values (year of publication in parentheses). Mobilities μ of the used samples are given in units of 10^6 cm^2/Vs .

cannot reach a definite conclusion. Experiments in an in-plane magnetic field may provide more insight. Numerical studies also indicate a spin-polarized state.^{9,28} If this is true, the $\nu = \frac{5}{2}$ state is most probably realized as the Pfaffian.¹⁵

The energy gap of the RIQHE state at $\nu = 2.57$ has similar values to our FQHE gaps but a stronger density dependence. A possible explanation is a larger intrinsic gap together with greater sensitivity to disorder.

Figure 4 compares our activation gaps at $\nu = \frac{5}{2}$ to other results from the literature. Mobilities are given next to each data point (for our data points, refer to Fig. 1). Some examples illustrate the large scatter in the data: first, compare our highest n data point with the result from Ref. 35. Density as well as mobility is considerably lower in our sample, however the measured gaps are similar. Then, comparing two $\mu = 28 \times 10^6$ cm^2/Vs samples from Refs. 21 and 22 having the same density, the gap differs by more than a factor of two. Probably the most striking example in this context is Ref. 19 and the $\mu = 28 \times 10^6$ cm^2/Vs sample from Ref. 21: density *and* mobility are increased by a factor of 2 for the latter, however, the activation gap is smaller. Also keeping in mind that, apart from the published data, many very high mobility wafers show a weaker $5/2$ state, these examples clearly illustrate that the mobility is a poor figure of merit to predict the quality of the $\nu = \frac{5}{2}$ state. In fact, a study of the influence of overdoping indicates that the FQHE is far more sensitive to RI than the electron mobility.³⁹ This may be related to the shorter correlation length of the RI disorder potential and will be discussed further below.

Comparing also the relative gap values of different second LL states, the results from different research groups show considerable irregularities: We find $5/2$ and $7/3$ to be of similar strength whereas $8/3$ is considerably weaker. This is partly consistent with (e.g., Refs. 19 and 21), partly in contrast to (e.g., Ref. 22: $\Delta_{7/3} \approx \Delta_{8/3} \approx \Delta_{5/2}$) previously reported results. The $11/5$ and $14/5$ states were reported to be stronger than $7/3$ and $8/3$, for instance, in Refs. 19 and 22 but are weaker in our sample. Also for the RIQHE the results from different groups yield a nonuniversal picture.^{19,35} These discrepancies again suggest that growth details, e.g., disorder, matter. Also the density-dependent degree of spin polariza-

tion may play some role. However, quantitative assertions about different gap values in the second LL should not be overrated since the experimentally accessible gaps are only a small part of the intrinsic gaps as we show below.

III. COMPARISON TO THEORY

The FQHE exists solely by virtue of the electronic Coulomb interaction and hence it is customary to normalize the energy gap $\Delta_{5/2}$ with the Coulomb interaction strength, $E_q = e^2/4\pi\epsilon\epsilon_0 l_B$. Here, $\epsilon = 12.9$ is the dielectric constant of GaAs and $l_B = (\hbar/eB)^{1/2}$ the magnetic length. However, we suggest here that the resulting dimensionless gap parameters $\tilde{\Delta}_{5/2} = \Delta_{5/2}/E_q$ should not be directly compared between different samples: the finite width of the electronic wave function as well as LL mixing effects influence the intrinsic energy gap considerably. The wave-function width depends on the design of the heterostructure and there is no clear-cut relation to density. The influence of LL mixing decreases with increasing density (at fixed ν), contrary to the Coulomb interaction strength. Both effects should therefore be taken into account explicitly when comparing activation gaps, as we do in this section for our density-tunable sample.

A. Ideal 2D system

The Hamiltonian to describe the two-dimensional electron system contains five contributions: the Coulomb interaction term, the kinetic-energy term, the confinement potential in the z direction, the external disorder potential, and a Zeeman term. We first address an idealized case: a strictly two-dimensional system without disorder and LL mixing. Also full spin polarization is assumed as valid for the Pfaffian and indicated by numerics.^{9,28} With these simplifications we are left with the Coulomb interaction term, from which we calculate the energy of a quasiparticle-quasihole exciton with maximal angular momentum for an N -electron system on a sphere with $N=8$ up to $N=20$. The quasiparticle (QP) and quasihole (QH) size is of order $12 l_B$ (see below and Ref. 45), which is large compared to the possible spacing on the sphere. We thus added the Coulomb energy necessary to bring the QP and QH infinitely apart. Furthermore, we investigated the contribution from the QP and QH quadrupole moments but found it to be negligible. By extrapolation to infinite systems as $1/N \rightarrow 0$ we obtain that the dimensionless gap parameter $\tilde{\Delta}_{5/2}$ equals 0.036. Within the accuracy of the extrapolation this is consistent with a value of 0.03 obtained from density-matrix renormalization-group techniques.¹²

Since the Coulomb interaction scales with the inverse of the electron distance the activation gap of the idealized system is proportional to the square root of the density: $\Delta_{5/2} \sim \sqrt{n}$. This is shown as Δ^{ideal} for our exact diagonalization result in Fig. 5(a). These calculated gaps are more than one order of magnitude larger than our experimental values Δ^{exp} .

B. Finite-width correction

We now consider corrections to the theoretical energy gaps due to (i) the finite width of the electronic wave

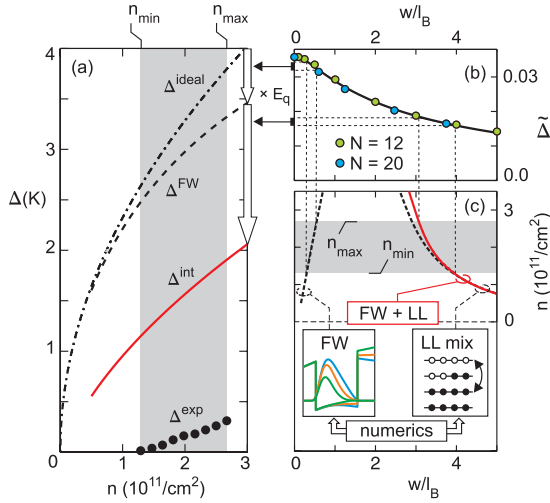


FIG. 5. (Color) (a) Comparison of our measured $5/2$ gaps to theory. See text for details. (b) Reduction in dimensionless gap parameter due to the normalized finite width w/l_B of the electronic wave function, obtained from exact diagonalization of up to 12 and 20 electrons. (c) Normalized finite width as a function of electron density. Left dashed line and inset: actual finite width. Right dashed line and inset: effective width due to Landau-level mixing. Solid red line: combined effect of FW and LL mixing.

function,^{14,46} (ii) Landau-level mixing,^{32,47} and (iii) disorder broadening. The electronic system is not strictly two-dimensional. Rather, the wave function Ψ has a finite extension perpendicular to the quantum well, as illustrated in the left inset of Fig. 5(c). In particular, when the average distance $d \sim l_B$ between electrons⁴⁸ is not large compared to the wave-function width w (measured by the standard deviation of $|\Psi|^2$), the Coulomb interaction is weakened. The dimensionless gap parameter $\tilde{\Delta}$ thus decreases with increasing w/l_B . We compute this effect by repeating the previously described exact diagonalization of finite systems for different w/l_B . The result is plotted in Fig. 5(b) (circles). In the shown w/l_B range we have approximately

$$\tilde{\Delta} = \frac{0.105}{2.59 + \sqrt{0.111 + (w/l_B)^2}}. \quad (1)$$

We obtain w as a function of density for our specific heterostructure from a self-consistent Poisson and Schrödinger solver.⁴⁹ The left inset at the bottom of panel (c) shows the wave function in the quantum well for three different back-gate voltages ($n=1.0, 1.8,$ and $2.7 \times 10^{11}/\text{cm}^2$). The single-sided doping results in an asymmetric quantum well at low densities with the wave function pushed against the upper GaAs-AlGaAs interface. For increasing n , the wave function broadens and is more centered.

Dividing the obtained widths by l_B yields the left dashed line in panel (c). The density range covered in our experiments is shaded. Going to panel (b) we obtain $\tilde{\Delta}$ including finite-width corrections.⁵⁰ Panel (a) shows the resulting gaps Δ^{FW} .

C. Landau-level-mixing correction

As a second correction, we take into account the effect of LL mixing within the random-phase approximation (RPA) as described in Ref. 32. It turns out that LL mixing causes a reduction in the Coulomb repulsion at short distances in a way very similar to the effects of the finite width of the wave function. By requiring that the Haldane pseudopotentials which include LL mixing within the RPA are accurately represented by those obtained for a 2D system with a suitably chosen effective width, it is easy to incorporate both finite width and LL mixing effects. The red solid curve in Fig. 5(c) shows the density dependence of w^{eff}/l_B incorporating both actual and effective finite-width effects for our specific heterostructure. In the displayed density range we have approximately

$$w^{\text{eff}}/l_B = 3.5n^{-0.25} + 0.9n^{-1}, \quad (2)$$

where n is in units of $10^{11}/\text{cm}^2$.

The right dashed curve in panel (c) shows the effective width due to LL mixing alone. In our sample the LL mixing corrections dominate over the actual finite-width corrections at $\nu = \frac{5}{2}$. This is not surprising in view of the rather small cyclotron energy at these values of the magnetic field. The ratio of the Coulomb and cyclotron energy characterizes the LL coupling strength. It scales as $1/\sqrt{B}$ and is of order unity for our experiment. Note that the actual and effective finite width are not additive. Nevertheless, as the actual width is only a small correction, Eq. (2) should be a good approximation for common heterostructure designs.

Going to panel (b) we see that the reduction in $\tilde{\Delta}$ is mainly the result of LL mixing effects and becomes more important at low densities. Finite-width effects only lead to smaller corrections that, however, increase with increasing density. Panel (a) shows the activation gap with both finite-width and LL-mixing corrections included as the intrinsic gap Δ^{int} . The corrections reduce the discrepancy between calculated gap and measured activation energy by about a factor of 2. At the largest density there is still about a factor of 6 difference. In absolute terms this difference is about 1.5 K.

D. Disorder and quasiparticle size

Finally, we address the influence of disorder. Due to the lack of theoretical treatments, disorder is often simply accounted for by a static level broadening Γ , with Γ as the difference between the intrinsic and the experimentally determined energy gap $\Gamma = \Delta^{\text{int}} - \Delta^{\text{exp}}$. Adopting this approach, we find that Γ increases slightly with density and reaches $\Gamma \approx 1.5$ K at the highest density. An estimate for the influence of disorder can also be extracted from the electron mobility and the quantum lifetime. The mobility yields a broadening of only 1 mK, the quantum lifetime gives 0.19 K which is still much smaller than the Γ extracted from $\Delta_{5/2}$ measurements. Similar discrepancies have been reported before.¹⁹ This is in line with the aforementioned indications (see Sec. II C) that the quality of FQHE is difficult to predict from the electron mobility. Disorder from the remote ionized

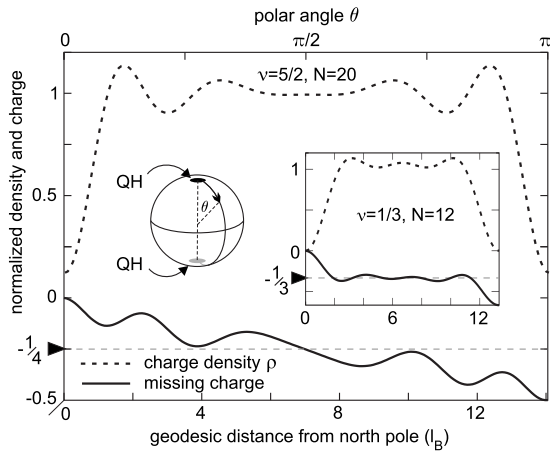


FIG. 6. To determine the size of quasiholes for $\nu = \frac{5}{2}$ and $1/3$ we put two quasiholes on a sphere occupied by $N=20$ and 12 electrons, respectively (left inset). The missing charge associated with the quasiholes is obtained from integration along the polar angle θ . For $1/3$ it levels at $2l_B$ from the poles (right inset). For $5/2$ no plateau is observed even for 20 electrons. The quasihole diameter is thus $\geq 12l_B$, which is about 150 nm at $B=4$ T.

donors, although of little relevance for the mobility in these heterostructures, seems to play a central role for the $5/2$ state.³⁹ We found the quantum lifetime to be limited by the RI as well, yet the broadening associated with τ_q is too small. It suggests that the current-carrying quasiparticles of the $5/2$ state are sensitive to different aspects of the disorder landscape than electrons in the weak-field regime. We return to this issue below. For the IQHE a more sophisticated way to treat disorder than a simple level broadening has been put forward: electrons move in a network of resistors formed by saddle points separating percolation clusters in the disorder potential landscape. The dissipative resistance originates from tunneling through these saddle points.³⁶ In contrast to the static level broadening model, the tunneling probability depends not only on the disorder landscape but also on the size of the tunneling particles. d'Ambrumenil⁵¹ has argued that the activation energy is substantially reduced if the quasiparticle size approaches or even exceeds the typical width of saddle points, which is on order of the spacer thickness in modulation-doped samples. An extension of this model to $\nu = \frac{5}{2}$ has to be worked out. Here, we investigate the $5/2$ QP and QH size: on a sphere occupied by $N=20$ electrons we localize two QHs on the north and south poles by a suitable pinning potential (left inset in Fig. 6) and numerically calculate the resulting charge density on the surface of the sphere. The diameter of the region of charge depletion will be interpreted as the size of the QH. Figure 6 shows the charge density ρ along the polar angle θ (dashed line). It has pronounced dips at the north and south poles where the QHs are located. To find the missing charge (solid line) we integrate $(\rho-1)\sin\theta$, along the polar angle θ . For the $5/2$ state we expect $-1/4$ for each QH. The missing charge has not yet settled at the equator. Hence, the true radius of the QH cannot be determined with confidence from exact calculations limited to 20 electrons on a sphere. Larger systems would be needed. However, it is possible to give a lower bound: as no

plateau is observed in the missing charge, the QH radius clearly exceeds $6l_B$. Also our exact diagonalization results for varying strength of the pinning potential used to localize the QHs at the north and south poles give a lower bound of $4l_B$ for the radius. Taking $12l_B$ as the QH diameter and a typical field of 4 T, we find 155 nm. The size of a QP seems to be even larger than that of a QH. In contrast, at $\nu = 1/3$ the missing charge has settled at around $2l_B$, see right inset. Also $1/3$ is typically measured at much larger magnetic fields. For example, at 16 T, which corresponds to $n = 1.3 \times 10^{11} / \text{cm}^2$, the $1/3$ QH is only 26 nm in diameter. This is a factor of six smaller than the minimum size of the $5/2$ QH.

The size of the $5/2$ QP of at least 150 nm at 4 T is larger than the spacer thickness in our heterostructure (66 nm) and thus the length scale of saddle points in the RI disorder landscape. This facilitates tunneling through saddle points and reduces the activation energy and can thus explain the large discrepancy between theory and experiment. Also, the activation-energy reduction due to tunneling is expected to be a certain fraction of the intrinsic gap. Our results lie just between this prediction and a constant reduction that a level broadening model would suggest. A possible explanation is better disorder screening for higher densities. Thus, the surprisingly large size of $5/2$ QP can qualitatively explain the large discrepancy between our measured $5/2$ gaps and theory. It can also explain that this discrepancy is larger than suggested by the quantum lifetime, even though τ_q is limited by the same type of disorder, namely, the remote ionized impurities.

IV. SUMMARY

We theoretically calculated the activation energy for the $\nu = \frac{5}{2}$ state by exact diagonalization for the experimentally relevant electron-density range. We included corrections due to finite width of the wave function and LL mixing. We found LL mixing to be the far more important correction. A state-of-the-art heterostructure with variable density was used to experimentally obtain the activation energy. The measured values are about 1.5 K below our theoretical prediction. The disorder broadening calculated from the transport mobility is three orders of magnitude less than this energy difference between theory and experiment. There is also no apparent correlation between the electron mobility and the size of the activation gap. Hence, the electron mobility is a poor figure of merit to assess the quality of the $5/2$ state and this state seems to be affected much more from remote ionized impurities in the donor layer than from background impurities.

Even though our study suggests that both the quantum lifetime and the $5/2$ gap are mainly influenced by remote ionized impurities, the broadening derived from the quantum lifetime is still five times smaller than the deviation of the experimental gaps from their theoretical values. In an effort to elucidate this discrepancy, we investigated the size of the quasiparticles of the $5/2$ state. These quasiparticles were found to be surprisingly large: the diameter exceeds $12l_B$ or 150 nm at a magnetic field of 4 T. This is larger than the length scale of the RI disorder potential set by the spacer

thickness, i.e., the separation of the ionized impurities from the 2DES. For the sake of completeness, we note that the average distance between background impurities is estimated to be about 500 nm.

At a qualitative level a natural explanation for the discrepancy in the gap values between theory and experiment may be provided by the extension of a quantum-tunneling model to the FQHE. This model has been put forward in the integer quantum-Hall regime to describe the influence of disorder beyond the oversimplified static level broadening picture. In this model quasiparticles need to tunnel through saddle points of the potential landscape to produce dissipative resistance. The geometric scale of the saddle points is determined by the spacer thickness. The large size of the $5/2$ quasiparticles would facilitate such tunneling events and reduce the activation energy. This can qualitatively explain the large discrepancy between theory and experiment.

Our results suggest that samples with larger spacers are needed to reduce the detrimental impact of disorder on the $5/2$ activation energy because the relevant disorder length

scale increases with the spacer thickness. The larger the ratio of disorder length scale to quasiparticle size is,⁵² the more tunneling across saddle points will be suppressed and consequently the activation energy will be increased.

The size of the $5/2$ quasiparticles is found to be of the same order of magnitude as the characteristic features of quantum-point contacts^{18,24} and interferometer nanostructures²⁵ designed to control them in experiments toward topological quantum computation. This likely is important for the proper interpretation of data obtained on such devices.

ACKNOWLEDGMENTS

We acknowledge helpful discussions with B. Rosenow, M. Storni, and N. d'Ambrumenil as well as financial support from GIF, ISF, DIP, Minerva foundation, European Research Council, U.S.-Israel Bi-National Science Foundation and the BMBF.

-
- ¹R. Willett, J. P. Eisenstein, H. L. Stormer, D. C. Tsui, A. C. Gossard, and J. H. English, *Phys. Rev. Lett.* **59**, 1776 (1987).
- ²W. Pan, J.-S. Xia, V. Shvarts, D. E. Adams, H. L. Stormer, D. C. Tsui, L. N. Pfeiffer, K. W. Baldwin, and K. W. West, *Phys. Rev. Lett.* **83**, 3530 (1999).
- ³S. Das Sarma, M. Freedman, and C. Nayak, *Phys. Rev. Lett.* **94**, 166802 (2005).
- ⁴P. Bonderson, A. Kitaev, and K. Shtengel, *Phys. Rev. Lett.* **96**, 016803 (2006).
- ⁵A. Stern and B. I. Halperin, *Phys. Rev. Lett.* **96**, 016802 (2006).
- ⁶C. Töke and J. K. Jain, *Phys. Rev. Lett.* **96**, 246805 (2006).
- ⁷M. Levin, B. I. Halperin, and B. Rosenow, *Phys. Rev. Lett.* **99**, 236806 (2007).
- ⁸S. S. Lee, S. Ryu, C. Nayak, and M. P. A. Fisher, *Phys. Rev. Lett.* **99**, 236807 (2007).
- ⁹I. Dimov, B. I. Halperin, and C. Nayak, *Phys. Rev. Lett.* **100**, 126804 (2008).
- ¹⁰G. Möller and S. H. Simon, *Phys. Rev. B* **77**, 075319 (2008).
- ¹¹X. Wan, Z. Hu, E. H. Rezayi, and K. Yang, *Phys. Rev. B* **77**, 165316 (2008).
- ¹²A. E. Feiguin, E. Rezayi, C. Nayak, and S. Das Sarma, *Phys. Rev. Lett.* **100**, 166803 (2008).
- ¹³B. Rosenow, B. I. Halperin, S. H. Simon, and A. Stern, *Phys. Rev. Lett.* **100**, 226803 (2008).
- ¹⁴M. R. Peterson, T. Jolicoeur, and S. Das Sarma, *Phys. Rev. Lett.* **101**, 016807 (2008).
- ¹⁵M. Storni, R. H. Morf, and S. Das Sarma, arXiv:0812.2691v2 (unpublished).
- ¹⁶N. R. Cooper and A. Stern, *Phys. Rev. Lett.* **102**, 176807 (2009).
- ¹⁷M. Baraban, G. Zikos, N. Bonesteel, and S. H. Simon, *Phys. Rev. Lett.* **103**, 076801 (2009).
- ¹⁸J. B. Miller, I. P. Radu, D. M. Zumbühl, E. M. Levenson-Falk, M. A. Kastner, C. M. Marcus, L. N. Pfeiffer, and K. W. West, *Nat. Phys.* **3**, 561 (2007).
- ¹⁹C. R. Dean, B. A. Piot, P. Hayden, S. Das Sarma, G. Gervais, L. N. Pfeiffer, and K. W. West, *Phys. Rev. Lett.* **100**, 146803 (2008).
- ²⁰C. R. Dean, B. A. Piot, P. Hayden, S. Das Sarma, G. Gervais, L. N. Pfeiffer, and K. W. West, *Phys. Rev. Lett.* **101**, 186806 (2008).
- ²¹W. Pan, J. S. Xia, H. L. Stormer, D. C. Tsui, C. Vicente, E. D. Adams, N. S. Sullivan, L. N. Pfeiffer, K. W. Baldwin, and K. W. West, *Phys. Rev. B* **77**, 075307 (2008).
- ²²H. C. Choi, W. Kang, S. Das Sarma, L. N. Pfeiffer, and K. W. West, *Phys. Rev. B* **77**, 081301(R) (2008).
- ²³M. Dolev, M. Heiblum, V. Umansky, A. Stern, and D. Mahalu, *Nature (London)* **452**, 829 (2008).
- ²⁴I. P. Radu, J. B. Miller, C. M. Marcus, M. A. Kastner, L. N. Pfeiffer, and K. W. West, *Science* **320**, 899 (2008).
- ²⁵R. L. Willett, L. N. Pfeiffer, and K. W. West, *Proc. Natl. Acad. Sci. U.S.A.* **106**, 8853 (2009).
- ²⁶G. Moore and N. Read, *Nucl. Phys. B* **360**, 362 (1991).
- ²⁷M. Greiter, X. G. Wen, and F. Wilczek, *Nucl. Phys. B* **374**, 567 (1992).
- ²⁸R. H. Morf, *Phys. Rev. Lett.* **80**, 1505 (1998).
- ²⁹E. H. Rezayi and F. D. M. Haldane, *Phys. Rev. Lett.* **84**, 4685 (2000).
- ³⁰S. Das Sarma, M. Freedman, and C. Nayak, *Phys. Today* **59**, 32 (2006).
- ³¹C. Nayak, S. H. Simon, A. Stern, M. Freedman, and S. Das Sarma, *Rev. Mod. Phys.* **80**, 1083 (2008).
- ³²R. Morf and N. d'Ambrumenil, *Phys. Rev. B* **68**, 113309 (2003).
- ³³J. P. Eisenstein, R. L. Willett, H. L. Stormer, and K. W. West, *Surf. Sci.* **229**, 31 (1990).
- ³⁴W. Pan, H. L. Stormer, D. C. Tsui, L. N. Pfeiffer, K. W. Baldwin, and K. W. West, *Solid State Commun.* **119**, 641 (2001).
- ³⁵J. P. Eisenstein, K. B. Cooper, L. N. Pfeiffer, and K. W. West, *Phys. Rev. Lett.* **88**, 076801 (2002).
- ³⁶D. G. Polyakov and B. I. Shklovskii, *Phys. Rev. Lett.* **74**, 150 (1995).

- ³⁷T. Baba, T. Mizutani, and M. Ogawa, Jpn. J. Appl. Phys. **22**, L627 (1983).
- ³⁸K.-J. Friedland, R. Hey, H. Kostial, R. Klann, and K. Ploog, Phys. Rev. Lett. **77**, 4616 (1996).
- ³⁹V. Umansky, M. Heiblum, Y. Levinson, J. Smet, J. Nuebler, and M. Dolev, J. Cryst. Growth **311**, 1658 (2009).
- ⁴⁰E. H. Hwang and S. Das Sarma, Phys. Rev. B **77**, 235437 (2008).
- ⁴¹V. Umansky, R. de Picciotto, and M. Heiblum, Appl. Phys. Lett. **71**, 683 (1997).
- ⁴²S. J. MacLeod, K. Chan, T. P. Martin, A. R. Hamilton, A. See, A. P. Micolich, M. Aagesen, and P. E. Lindelof, Phys. Rev. B **80**, 035310 (2009).
- ⁴³M. O. Goerbig, P. Lederer, and C. M. Smith, Phys. Rev. B **69**, 115327 (2004).
- ⁴⁴G. A. Csathy, J. S. Xia, C. L. Vicente, E. D. Adams, N. S. Sullivan, H. L. Stormer, D. C. Tsui, L. N. Pfeiffer, and K. W. West, Phys. Rev. Lett. **94**, 146801 (2005).
- ⁴⁵S. Das Sarma and R. Morf, the $\nu=\frac{5}{2}$ Qubit, KITP, LOWDIM09 workshop at KITP, lecture online: <http://online.itp.ucsb.edu/online/lowdim09/nu52/>
- ⁴⁶R. H. Morf, N. d'Ambrumenil, and S. Das Sarma, Phys. Rev. B **66**, 075408 (2002).
- ⁴⁷W. Bishara and C. Nayak, Phys. Rev. B **80**, 121302(R) (2009).
- ⁴⁸For $\nu=\frac{5}{2}$ one has $d=\sqrt{2\pi/\tilde{\nu}}l_B$ with $\tilde{\nu}=1/2$ as only the electrons in the half-filled second LL take part in the correlated state.
- ⁴⁹Nanodevice simulator, Spinoff from WSI, TU Munich, Germany, <http://www.nextnano.de/nextnano>
- ⁵⁰The gap is reduced by an increasing amount as density increases. This is, however, only partly due to increasing width w : as $l_B \sim 1/\sqrt{n}$, even a constant w would yield an increasing w/l_B and reduce the normalized gaps.
- ⁵¹N. d'Ambrumenil, Conference on strongly correlated low-dimensional systems, Ascona, July 2006 (unpublished).
- ⁵²Without a BG the achievable density n drops inversely proportional to spacer thickness d . Nevertheless, as $l_B \sim 1/\sqrt{n}$, the QP size increases only as \sqrt{d} , thus slower than the disorder length scale.